

# Unraveling PROTAC Mechanisms Through Biophysical Profiling

From DNA-encoded Library to Cellular Degradation

## Abstract

Targeted protein degradation (TPD) has rapidly advanced as a new therapeutic modality, with PROTACs standing out as the leading and most broadly applied approach. To fully harness the therapeutic potential of PROTACs, a systematic workflow that integrates biophysical characterization is essential for understanding E3 ligase recruitment and ternary complex formation, key determinants of degradation efficiency and selectivity. To this end, a prototypical workflow for PROTAC design and characterization is presented here, employing BRD4 as a model target and combining comprehensive biophysical and cellular analyses. Binders selective for bromodomain 1 of BRD4 were initially identified via DNA-encoded library (DEL) screening, and PROTAC molecules were subsequently designed to recruit the E3 ligase Cereblon (CRBN). Binary binding kinetics across various BRD4 constructs and PROTAC variants were determined by surface plasmon resonance (Triceratops SPR #64), providing insights into PROTAC specificity, while ternary complex formation was evaluated and validated using **switchSENSE**<sup>®</sup> technology and the recently developed Y-structure proximity assay, yielding important information on the complex binding mechanism. Importantly, the results of these biophysical analyses were supported by cellular studies, which demonstrated clear evidence of BRD4 ubiquitination and subsequent degradation, highlighting the functional relevance of the PROTAC-induced mechanism in a cellular context.

By integrating high-resolution biophysical profiling with cellular degradation assays, detailed mechanistic insights into PROTAC mode of action were obtained, laying the foundation for data-driven optimization of degrader candidates.

## Keywords:

DNA-encoded library, DEL, PROTACs, CRBN, kinetics, SPR, binary affinities, **switchSENSE**, Y-structure, ternary complex formation, cellular degradation

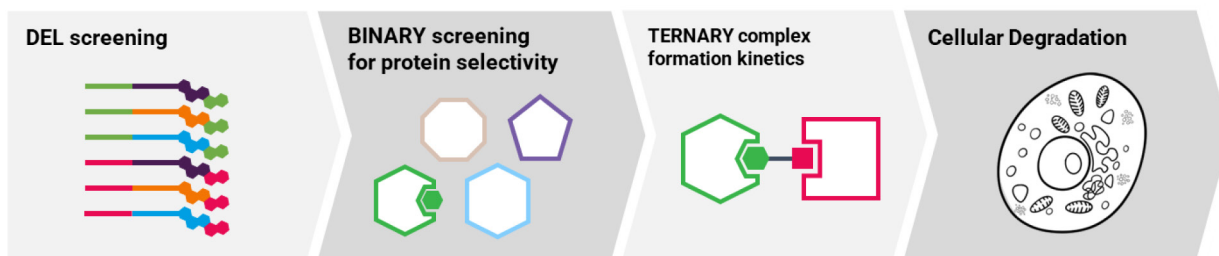


**Figure 1.** Workflow for the comprehensive biophysical PROTAC profiling from identification to cellular assays.

## Introduction

Proteolysis-Targeting Chimeras (PROTACs) have emerged as an innovative therapeutic modality that exploits the ubiquitin–proteasome system to induce selective protein degradation. These heterobifunctional molecules comprise a target-binding ligand and an E3 ligase–binding ligand, connected via a chemical linker.

The design of effective PROTACs involves several key challenges: the identification of high-affinity and selective ligands (warheads) for both the target protein and the E3 ligase; optimization of the linker to ensure appropriate spatial orientation; validation of a stable ternary complex with sufficient lifetime to enable ubiquitination; and demonstration of efficient protein degradation in a cellular environment. The latter is strongly influenced by the overall physicochemical properties of the molecule, particularly its cellular permeability, chemical stability, and size. Indeed, many PROTACs, often exceeding 800 Da, suffer from poor oral bioavailability, limited blood–brain barrier penetration, and suboptimal pharmacokinetics.

DNA-encoded library (DEL) screening offers a high-throughput approach to identify ligands from vast and chemically diverse small-molecule libraries. DEL-derived hits are particularly attractive starting points for PROTAC development, as the known exit vector (i.e., the attachment site of the DNA tag) can conveniently guide conjugation of the E3 ligase–recruiting moiety, thereby streamlining the design process. When combined with biophysical techniques to characterize binary binding kinetics and ternary complex formation, and with cellular degradation assays, this strategy provides a robust and integrated workflow for PROTAC discovery.

In this study, the development of PROTAC molecules targeting bromodomain 1 of BRD4, a model system and therapeutically relevant cancer target [1], and Cereblon (CRBN), one of the most widely used E3 ligases in PROTAC research due to its clinical validation [2], is reported. In particular, CRBN<sup>midi</sup>, a stabilized truncated construct developed by Kroupova et al. [3], was employed to enable high-resolution structural and biophysical characterization of both binary and ternary complexes.

### DNA-encoded library (DEL) screening

Discovery of novel ligands remains a critical step in the development of effective PROTACs targeting bromodomain proteins. Over recent decades, DEL screening has become a cornerstone technology in drug discovery due to its ability to rapidly explore a vast chemical space with libraries containing millions of compounds featuring optimized physicochemical properties and diverse chemotypes, beyond traditional high-throughput screening. This technology allows rapid identification of potent binders using minimal material in a single experiment. The combinatorial design of DELs facilitates extraction of structure-activity relationship (SAR) trends to guide lead optimization. Additionally, DEL screening can assess binding modes, distinguishing orthosteric from allosteric interactions, by employing competition assays with known bromodomain inhibitors like (+)JQ1. Following DNA tag decoding, selected ligands can be synthesized off-DNA for further validation and PROTAC development.

### Binary screening for protein selectivity

The penultimate prerequisite for any PROTAC is its capability to bind to the target protein via its warhead and to the ligase via the ligase-binding moiety. Warheads targeting protein families with several isoproteins such as the Bromodomain family raise the concerns of selectivity and thus potentially side-effects as well as different pharmacological effects [4]. Additionally, the linker attachment to a warhead might impede the binding affinities and kinetics to the target protein or of the ligase binding moiety to the target ligase. Finally, kinetic characterization of either interaction can indicate insufficient ternary complex formation. These aspects are most efficiently studied with

a biophysical, direct binding assay which is unaffected by biological aspects such as cell permeability and thus allows direct correlations of molecular changes to target engagement capabilities. Multiplexed Surface Plasmon Resonance (SPR) with the Triceratops SPR #64 allows the detailed characterization of kinetics, binding affinities and selectivity in a single experiment. Its rotatable manifold enables the measurement of up to 8 compounds against up to 8 proteins simultaneously in just few hours, saving time and material (Figure 2).

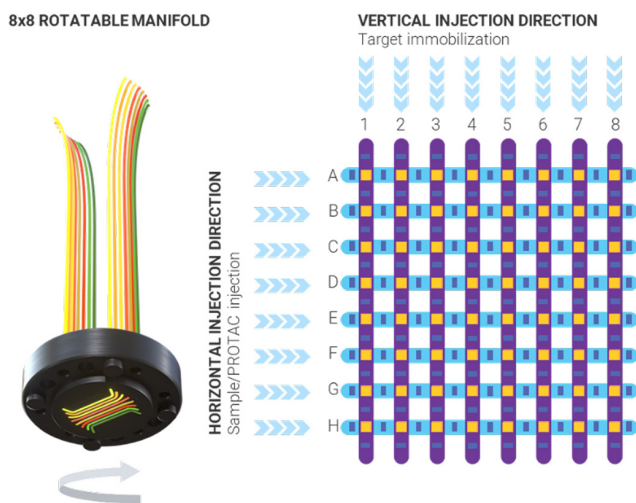


**Figure 2. Overview of the Triceratops SPR #64 rotatable manifold and sensor grid layout.** The grid comprises 64 active sensor spots (yellow squares), enabling simultaneous vertical immobilization of 8 targets (1–8; purple lines) and, after rotation, horizontal injection of 8 analytes (A–H; light blue lines) to generate an 8 × 8 kinetic matrix. In addition, 72 reference spots are included (dark blue).

### PROTAC ternary complex formation analysis

Ternary complexes, composed of two proteins bridged by small molecules such as PROTACs, pose unique challenges for the analysis of molecular interactions, as their behavior is governed not only by binary binding affinities but also by cooperativity and avidity effects. In this study, the newly established **switchSENSE**<sup>®</sup> proximity binding assay [5] was utilized to measure ternary interaction kinetics on a biosensor surface. In this setup, the target protein and the substrate-binding subunit of the ubiquitin E3 ligase were tethered in a 1:1 stoichiometry to the mobile swivel arms of a Y-shaped DNA scaffold (referred to as the Y-structure), thus positioning them in close proximity and enabling their engagement with PROTAC analytes flowing across the sensor. PROTAC-induced ternary complex formation was detected by fluorescence resonance energy transfer (FRET), while binary interactions were monitored via fluorescence proximity sensing (FPS), which yields a fluorescence quenching or anti-quenching signal upon binding (Figure 3).

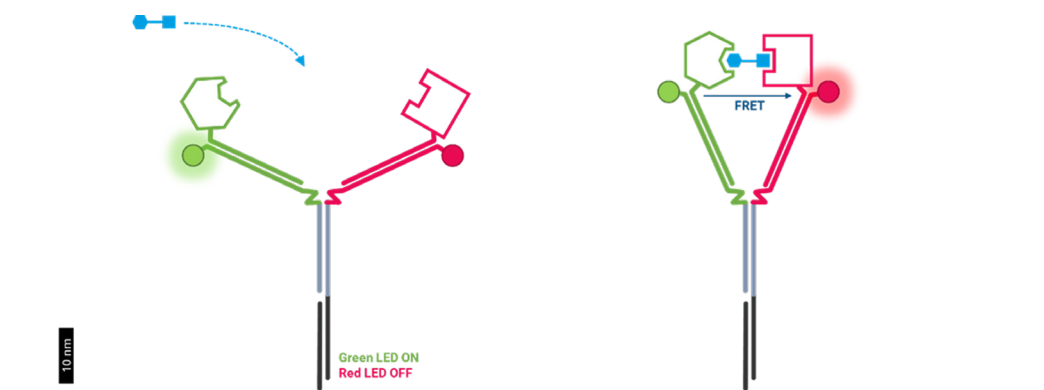


**Figure 3. Y-shaped DNA structure for proximity assays.** The Y-structure is made up of a stem and two swivel arms connected by flexible linkers and consists of four DNA strands. The protein-of-interest (POI) and E3 ligase substrate receptor (E3 ligase) are attached to the distal arm ends. Green and red fluorophores are attached to the distal ends of the swivel arms to detect binary binding via fluorescence quenching (FPS mode) and ternary binding via fluorescence energy transfer (FRET mode). A FRET signal is generated when the arms are closed.

## Cellular degradation study

An essential step toward advancing PROTAC development is the implementation of robust and quantitative degradation assays, which enable the assessment of degradation efficiency, selectivity, and kinetics within a cellular environment. Beyond confirming the cellular activity of PROTAC molecules, these assays provide critical insights into structure–activity relationships (SAR), degradation mechanisms, and potential off-target effects, thereby supporting the rational optimization of degrader design. Among the available methods, Homogeneous Time-Resolved Fluorescence (HTRF®)-based quantification offers a particularly sensitive and high-throughput-compatible approach for monitoring PROTAC-induced target degradation in live cells. By allowing direct and quantitative detection of protein levels under physiological conditions, HTRF assays serve as a versatile tool for early-stage screening, potency ranking, and mechanistic characterization, bridging the gap between biochemical ternary complex studies and cellular degradation outcomes. In this study, an HTRF assay was employed to assess the cellular degradation efficiency of BRD4-targeting PROTACs by quantifying endogenous BRD4 levels in HeLa cells.

## Results and Discussion

### Screening with DNA-Encoded Library & design of PROTAC degraders

DEL screening was performed using a representative subset of NovAliX proprietary DNA-encoded libraries, covering more than 30 million compounds. The screening was performed on BRD4 BD1-BD2 Y309A: this mutation was reported to impair compound binding to BD2 [5], hence promoting the selection of BD1-selective compounds. About 500 compounds were selected based on their favorable enrichment and copy number (Figure 4). 8 hits were tested in off-DNA validation using TR-FRET competition assay and SPR for affinity estimation. Of those, one showed micromolar affinity for BRD4 BD1 as well as selectivity for BD1 over BD2 and was consequently selected for PROTAC transformation. No further optimization of the BRD4-binding moiety was performed, due to its favorable ADME parameters and physicochemical properties.

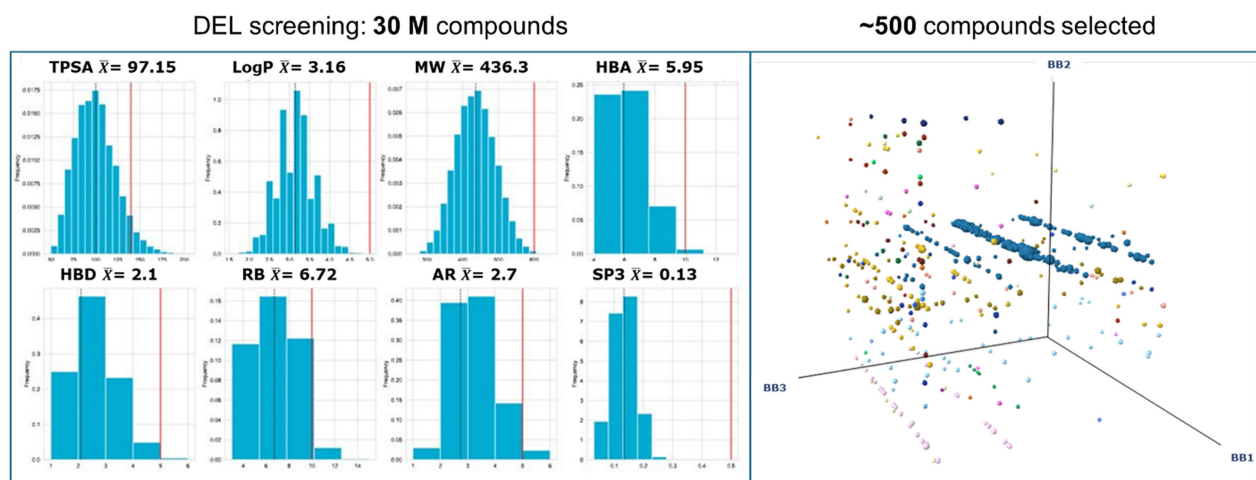


**Figure 4.** DEL screening against BRD4 BD1-BD2 Y309A protein. Left: physicochemical properties of the DEL library. Right: frequency of building blocks among the selected compounds. Clusters aligned along the BB1 axis indicate that a specific subset of building blocks was consistently enriched in the structures of the identified ligands.

**Table 1. Physicochemical properties of the 8 hits selected for off-DNA synthesis.**

HIT	Enrichment	PhysChem Properties				
		MW (Da)	HBD*	HBA**	logP***	tPSA****
HIT 1	12102	406	1	7	1,1	89
HIT 2	6799	470	2	5	2,9	100
HIT 3	5579	456	2	5	2,7	100
HIT 4	2550	394	1	9	0,2	98
HIT 5	1859	368	1	7	0,4	80
HIT 6	535	467	2	8	1,7	102
HIT 7	488	470	3	8	1,8	109
HIT 8	443	430	1	8	1,2	89

\*HBD (Hydrogen Bond Donors)

\*\*HBA (Hydrogen Bond Acceptors)

\*\*\*logP (Partition Coefficient)

\*\*\*\*tPSA (Topological Polar Surface Area)

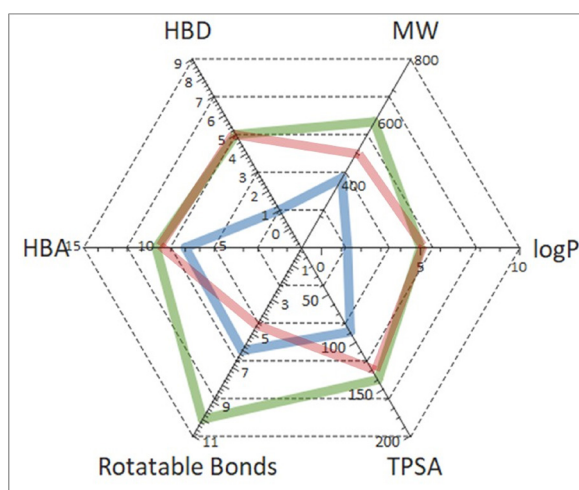


**Figure 5.** Physicochemical properties of the selected BRD4-binding moiety (Hit 1 in Table 1). Parameters associated with Lipinski's rule are indicated in red, NovaDEL criteria in green, and BRD4-binding moiety parameters in blue.

**Table 2.** Short description of the linker type used to create PROTAC molecules from hit 1.

PROTAC ID	Type of linker
PROTAC 1	Middle chain aliphatic (5C)
PROTAC 2	Middle chain aliphatic (8C)
PROTAC 3	Middle chain aliphatic (7C)
PROTAC 4	Short aliphatic (2C)
PROTAC 5	Middle chain bicyclic basic
PROTAC 6	Short aliphatic (3C)
PROTAC 7	Short mono cyclic

A set of 16 PROTACs, targeting either the CRBN substrate receptor or the VHL E3 ligase and incorporating different types of linkers, was consequently generated. After excluding compounds with low or no BRD4 potency in a TR-FRET assay, 7 CRBN-targeting molecules were selected. As listed in Table 2, these 7 PROTAC molecules cover a certain structural diversity, with linkers containing aliphatic chains of 2 to 5 carbon atoms, mono- or bicyclic structures, and different anchoring points.

### Selectivity study: multiplexed SPR binary characterization using Triceratops SPR #64

The Triceratops SPR#64 system was used for in-depth binary interaction analysis of the obtained designs. Both the binary interaction with the main target proteins, BRD4 and CRBN<sup>midi</sup>, and potential off-targets, BRD2 and BRD3, were characterized in a single experiment in about 30 hours runtime. Seven PROTAC designs together with MZ1 as control were measured against the single binding domains of BRD2, BRD3 and BRD4, the BD1-BD2 combined BRD4 construct and CRBN<sup>midi</sup> as E3 ligase. MZ1 exhibited the expected behavior described by Ciulli [7, 8] in terms of affinities and selectivity profiles except for BRD3-BD1 which could be caused by the different immobilization procedure. As expected, MZ1 also did not bind to CRBN<sup>midi</sup>.

The seven PROTACs generally showed a higher affinity to BD1 of BRD4 compared to BD2 with affinities ranging from 10 to 590 nM. Except for PROTAC 2, all designs have a more than 10-fold higher affinity to BD1. The affinities to BD1 or the full construct are similar, indicating that BD1 is the more relevant binding site for these designs.

Affinities to CRBN<sup>midi</sup> were a bit weaker ranging from 120 to 5.4  $\mu$ M. Of specific interest is PROTAC 4 which showed the highest affinity to BRD4 but has a more than 40-fold lower affinity to CRBN<sup>midi</sup>. The ten-fold higher off-rate of PROTAC 4 to CRBN<sup>midi</sup> compared to the other PROTACs further indicates clear differences in the interaction with CRBN<sup>midi</sup>. The shorter linker of PROTAC 4 could be limiting the necessary rotational freedom for the ligase-binding motif and thus hinder the interaction with CRBN decisively. Similarly, PROTAC 6 showed an even lower affinity to CRBN<sup>midi</sup> whilst having an affinity towards BRD4-BD1 comparable to that of PROTAC 2 and 3. The low affinity to the ligase might also be caused by a shorter linker.

A cross-family selectivity analysis (Figure 6 and 7) shows that all seven designs are comparably unselective towards BRD2-BD1. The selectivity ratios ( $K_d$  BRD2-BD1 /  $K_d$  BRD4-BD1) range between 1 and 5. It can thus be expected that BRD2-degradation may occur as well. PROTAC 1, 3 and 6 did not display any binding to BRD2-BD2 or BRD3 at all, indicating a more selective interaction profile. Similarly, PROTAC 4 and 7 do not bind BRD3, but it binds to the two domains of BRD2 at similar affinities, albeit at faster kinetics to BD1. PROTACs 2 and 5 show binding to the complete BRD-family. PROTAC 2 is the least selective compound with selectivity ratios of 10-15 for BRD2-BD2 and BRD3 (both BD1 and BD2) compared to BRD4-BD1. PROTAC 5 shows a clearer selectivity profile with affinities being up to 100-fold lower compared to BRD4-BD1.

**Table 3. Affinities determined from the binary interaction of the positive control Mz1 and the seven PROTAC-designs against the BRD-protein family panel and CRBN<sup>midi</sup>. Values are reported in nM. Non-binding is represented with the abbreviation "N.B."**

	BRD2		BRD3		BRD4			CRBN <sup>midi</sup>
	BD1	BD2	BD1	BD2	BD1	BD2	BD1/2	
<b>MZ1</b>	88	17	17400	2310	27	18	32	N.B.
<b>PROTAC 1</b>	340	N.B.	N.B.	N.B.	270	3090	200	530
<b>PROTAC 2</b>	940	3840	5560	4240	360	1780	320	120
<b>PROTAC 3</b>	750	N.B.	N.B.	N.B.	590	5730	520	210
<b>PROTAC 4</b>	33	52	N.B.	N.B.	9	940	13	440
<b>PROTAC 5</b>	390	5670	4300	7670	75	2480	23	230
<b>PROTAC 6</b>	480	N.B.	N.B.	N.B.	390	13700	390	5400
<b>PROTAC 7</b>	1110	170	N.B.	N.B.	740	7700	730	230

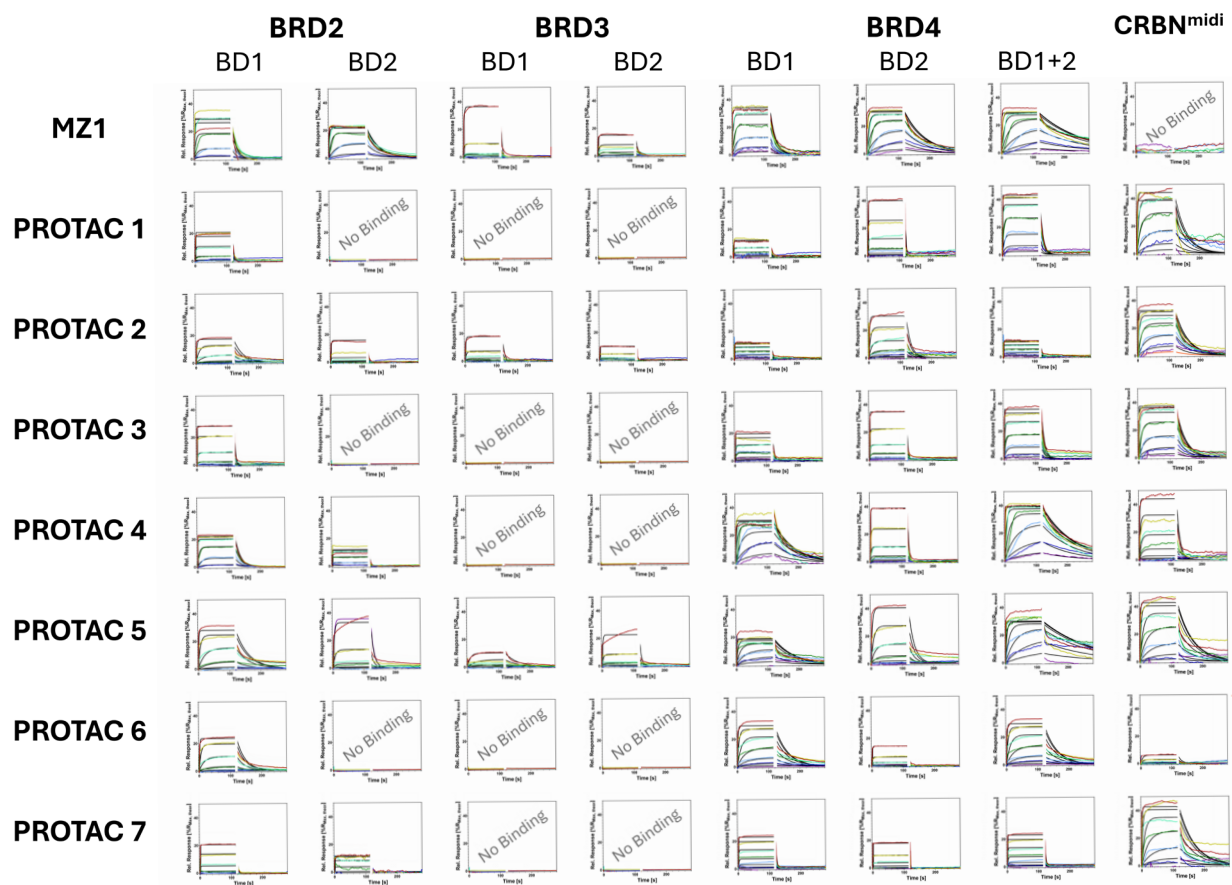


**Figure 6.** Kinetic screening of 64 interactions. Overview of all 64 multi-injection cycle kinetics (MICK) sensorgrams for MZ1 and seven PROTAC designs tested against the full set of BRD proteins and CRBN<sup>mid</sup>. Eight targets were immobilized vertically: (1) BRD2-BD1, (2) BRD2-BD2, (3) BRD3-BD1, (4) BRD3-BD2, (5) BRD4-BD1, (6) BRD4-BD2, (7) BRD4-BD1-BD2, and (8) CRBN<sup>mid</sup>; eight analytes were injected horizontally, producing an 8 × 8 kinetic matrix. Concentration series ranged from 8 μM with threefold dilutions across eight concentrations.

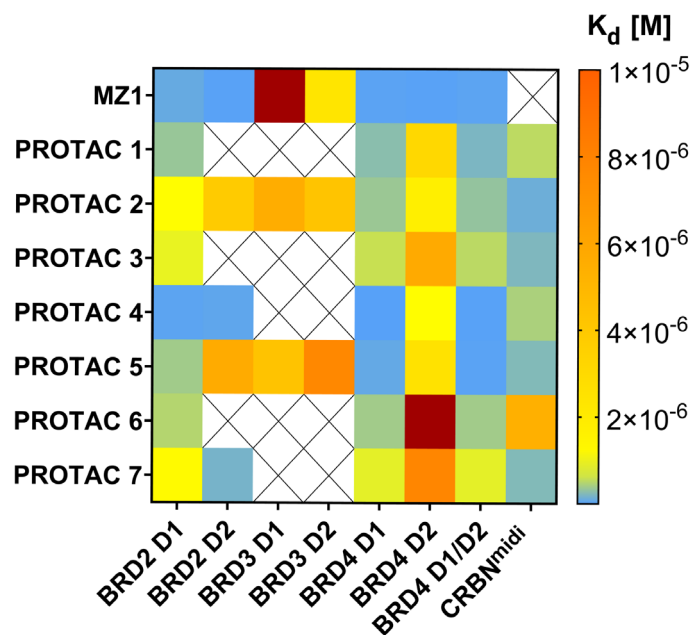


**Figure 7.** Heat map of binary affinities for all compounds. The 8 × 8 matrix corresponds to the 64 sensorgrams shown previously.  $K_d$  values are reported in M; warmer colors indicate weaker interactions, while white fields (X) denote conditions with no detectable binding. Affinity constants are summarized in Table 3.

## Ternary complex formation: kinetic characterization and validation of the binding mechanism

To assess PROTAC-mediated ternary complex formation, the previously described Y-structure was functionalized with the target protein BRD4-BD1 on the green-dye arm and the E3 ligase CRBN<sup>midi</sup> on the red-dye arm. BRD4-BD2 was also tested as a negative control for ternary complex formation. Fluorescence was excited in the green channel, while emissions from both channels were recorded simultaneously. Upon PROTAC injection, red emission was observed via green-to-red FRET as the Y-structure closed, indicating bridging of the target protein (BRD4) and ligase by the PROTAC. Upon PROTAC dissociation, the arms returned to the open state, and fluorescence in both channels recovered to baseline. Binary binding of the PROTACs to BRD4-BD1 was additionally monitored using fluorescence proximity sensing (FPS).

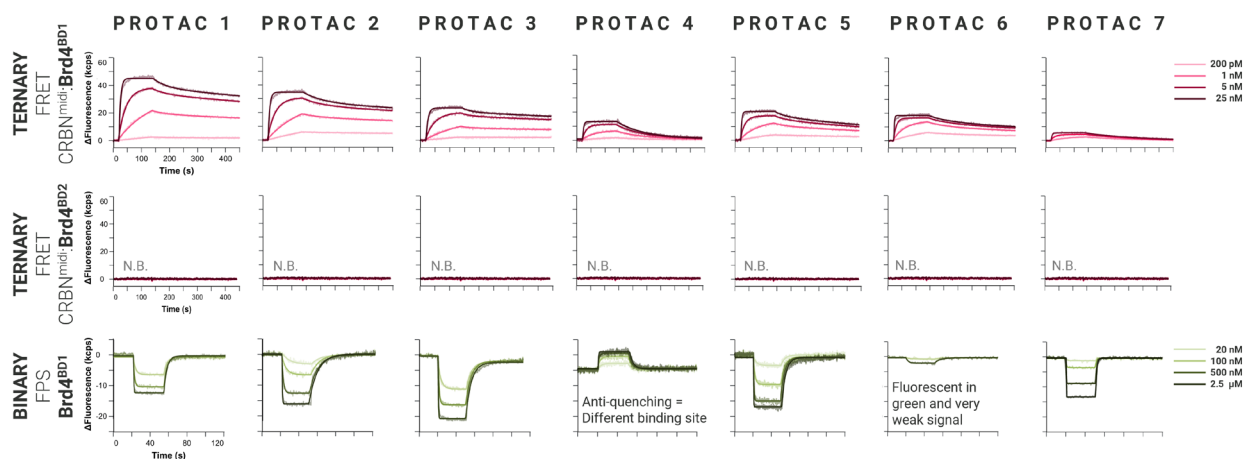


**Figure 8. Kinetic characterization of binary and ternary binding for the seven PROTACs.** Top and middle panels show red FRET signals from ternary complex formation with CRBN<sup>midi</sup> and BRD4-BD1 or BD2, respectively, measured upon green excitation at 0.2, 1, 5, and 25 nM PROTAC (N.B. indicates no binding detected). Green channel not shown here. Bottom panel shows binary binding to BRD4-BD1 measured in FPS (green) at 20, 100, 500 nM, and 2.5 μM PROTAC.

As shown in Figure 8, all PROTACs form ternary complexes with BRD4-BD1, whereas none show ternary complex formation with BRD4-BD2, consistent with the intended design. In detail, PROTACs 1, 2, and 3 display highly similar behavior, forming tight ternary complexes with BRD4-BD1 and CRBN<sup>midi</sup>, with dissociation constants in the high picomolar range. These compounds also exhibit strong and comparable binary binding to BRD4-BD1. PROTAC 5 forms a ternary complex of comparable affinity, albeit with slightly faster association and dissociation kinetics (Figure 9). PROTAC 6 also forms a relatively stable ternary complex; however, its binary binding to BRD4-BD1 is weak, as indicated by minimal fluorescence quenching. This behavior suggests an alternative binding mode to BRD4-BD1, likely influenced by its short linker chemistry.

In contrast, PROTAC 7 shows strong fluorescence quenching and rapid binary binding kinetics, yet forms only a weak and transient ternary complex, with a dissociation rate approximately tenfold faster than that of PROTAC 3.

Finally, PROTAC 4 forms the weakest ternary complex, with a dissociation rate nearly twentyfold faster than that of PROTAC 3. Notably, whereas all other PROTACs induce fluorescence quenching upon binding to BRD4-BD1, PROTAC 4 generates an anti-quenching signal, indicating a distinct binding mode or conformational response. This behavior is likely attributable to its very short linker, which may hinder or destabilize the overall ternary complex formation.

To further investigate this effect, origami nanolever [switchSENSE](#)<sup>®</sup> measurements were employed to probe protein conformational changes upon PROTAC binding to BRD4-BD1. The results (Figure 9) show that PROTAC 4 reproducibly induces pronounced protein compaction, as evidenced by a clear reduction in nanolever velocity. In contrast, the other PROTACs—illustrated by PROTAC 3 as a representative example—do not induce significant conformational changes and display comparable behavior.

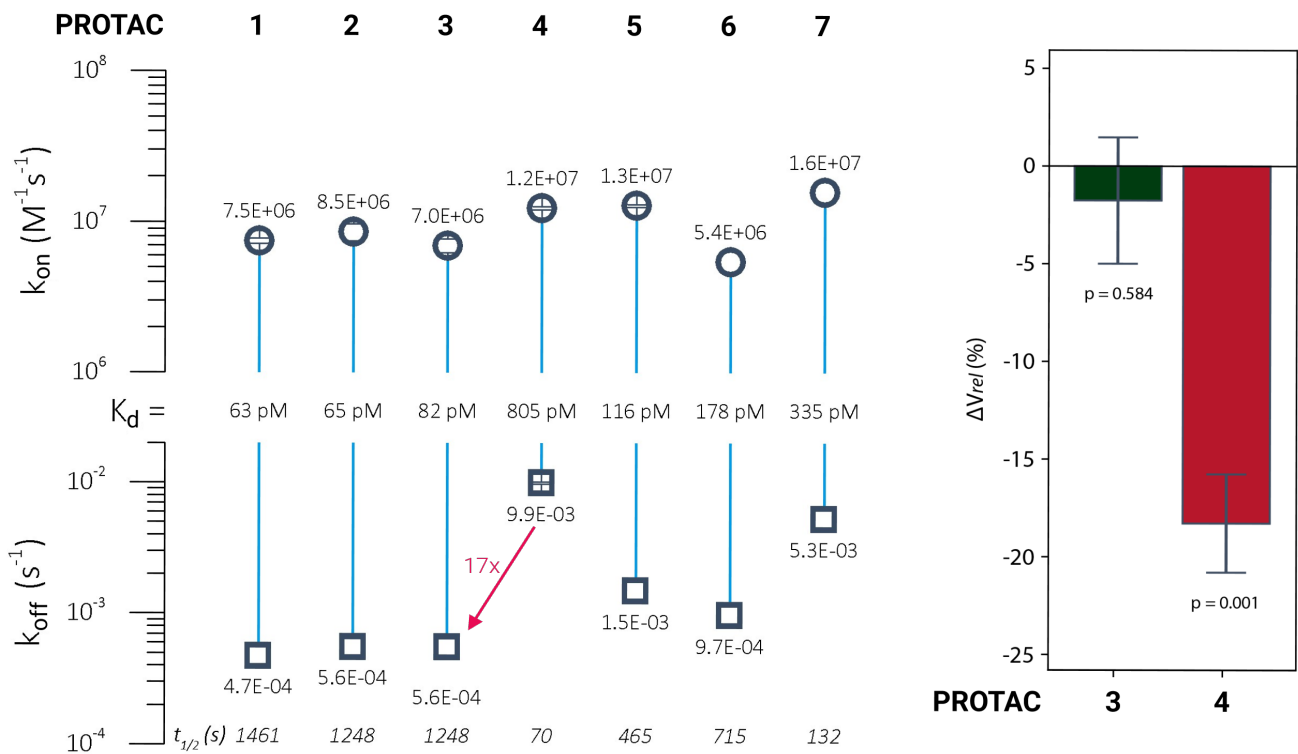


**Figure 9. Rate-scale plot and conformational change study.** Left: Rate-scale plot summarizing association ( $k_{on}$ ) and dissociation ( $k_{off}$ ) rate constants, as well as dissociation constants ( $K_d$ ), for ternary interactions of all seven PROTACs. Data represent the mean of two independent experiments. Right: Switching velocity of BRD4-BD1 upon binding of PROTAC 3 and PROTAC 4. Data are averaged from three independent measurements, real-time referenced, and p-values indicate high statistical significance.

### Degradation assay in HeLa cells

Quantification of endogenous BRD4 levels in HeLa cells revealed a marked reduction in protein abundance upon treatment with most of the previously described PROTACs. Specifically, PROTACs 2, 3, and 5 induced pronounced BRD4 degradation after 6 hours of treatment, displaying  $DC_{50}$  values in the micromolar range and maximal degradation ( $D_{max}$ ) exceeding 78%, shown in Table 4. In particular PROTAC 3 shows the highest degradation efficiency, which is most likely correlated with the slow dissociation rate from CRBN. PROTAC 1 showed substantially lower activity, with  $DC_{50}$  values above 5  $\mu M$  even after 24 hours of exposure, whereas PROTAC 7 exhibited only minimal degradation, with limited activity observed after 24 hours, in correlation with the relatively fast off-rate. PROTACs 4 and 6 failed to induce detectable BRD4 degradation. These results are consistent with **switchSENSE**<sup>®</sup> analyses, which showed that PROTACs 1, 2, 3, and 5 can form very stable ternary complexes, whereas PROTAC 4, due to a distinct conformational change in BRD4-BD1, hinders the ternary complex formation and consequently efficient degradation. Overall, BRD4 degradation was further enhanced at 24 hours with all active PROTACs.

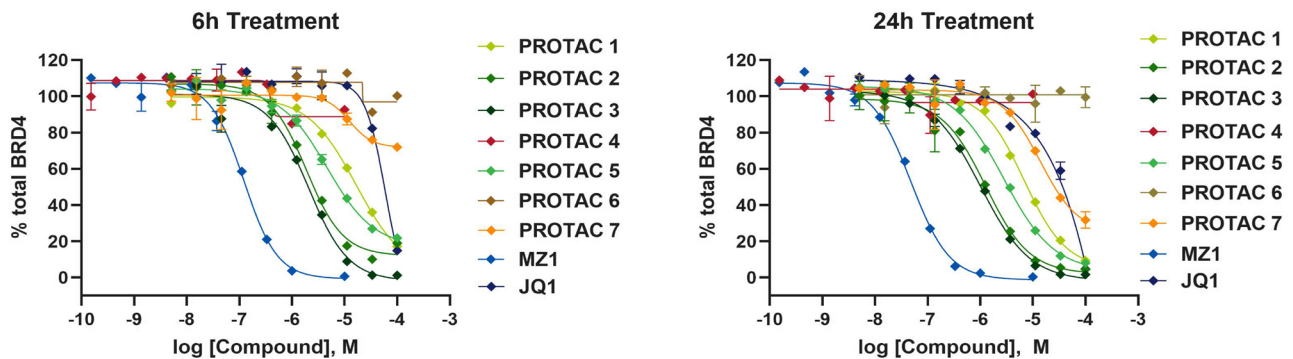


**Figure 10. HTRF-based assay measuring endogenous BRD4 degradation.** Dose response curves of 7 PROTACs, MZ1 PROTAC and JQ1 in HeLa cells at 6h and 24h of treatment. Data are reported as a percentage of BRD4 remaining.

**Table 4. Overview of resulting DC<sub>50</sub> and % of maximal Degradation (D<sub>max</sub>) obtained after 6h and 24h of treatment with 7 different PROTACs, assessing BRD4 degradation in HeLa cells.**

Compound	DC <sub>50</sub> (M), 6h treatment	D <sub>max</sub> <sup>r</sup> 6h treatment	DC <sub>50</sub> (M), 24h treatment	D <sub>max</sub> <sup>r</sup> 24h treatment
<b>PROTAC 1</b>	1.65E-05	83% at 100μM	6.79E-06	91% at 100μM
<b>PROTAC 2</b>	1.87E-06	90% at 33μM	1.27E-06	90% at 11μM
<b>PROTAC 3</b>	2.06E-06	98% at 33μM	1.00E-06	98% at 33μM, 94% at 11μM
<b>PROTAC 4</b>	>1.00E-04	8% at 10μM	>1.00E-04	absence of degradation up to 10μM
<b>PROTAC 5</b>	4.70E-06	78% at 100μM	2.81E-06	92% at 100μM
<b>PROTAC 6</b>	>1.00E-04	absence of degradation up to 100μM	>1.00E-04	absence of degradation up to 100μM
<b>PROTAC 7</b>	>1.00E-04	29% at 100μM	1.38E-05	68% at 100μM
<b>MZ1</b>	1.22E-07	99% at 10μM	4.67E-08	95% at 333nM
<b>JQ1</b>	5.98E-05	85% at 100μM	2.74E-05	96% at 100μM

### Ubiquitin-proteasome dependency of PROTAC-3-mediated BRD4 degradation

To further evaluate the PROTAC specificity, the mechanism of action of PROTAC 3 was investigated by demonstrating its dependency on the neddylation and proteasome pathways, as well as its recruitment of the Cereblon E3 ligase (CRBN). Using the same BRD4 HTRF assay, PROTAC 3 was tested in competition with the neddylation inhibitor MLN4924, the proteasome inhibitor MG132, and a CRBN ligand (Figure 11). BRD4 degradation in HeLa cells by PROTAC 3 is dependent on both the neddylation and proteasomal pathways. Co-treatment with the CRBN ligand rescues BRD4 levels, indicating that competition prevents formation of the ternary complex required for target degradation. The observed decrease in BRD4 levels upon treatment with PROTAC 3 at 10 and 100 μM (Figure 11, green bar) demonstrates its proteolytic activity. The inhibition of this degradation by a CRBN ligand, a proteasome inhibitor MG132, and a neddylation inhibitor MLN4924 confirms that BRD4 degradation is mediated by CRBN recruitment and the ubiquitin-proteasome system. Altogether, this evidence supports and validates the proposed mechanistic characterization of PROTAC 3.

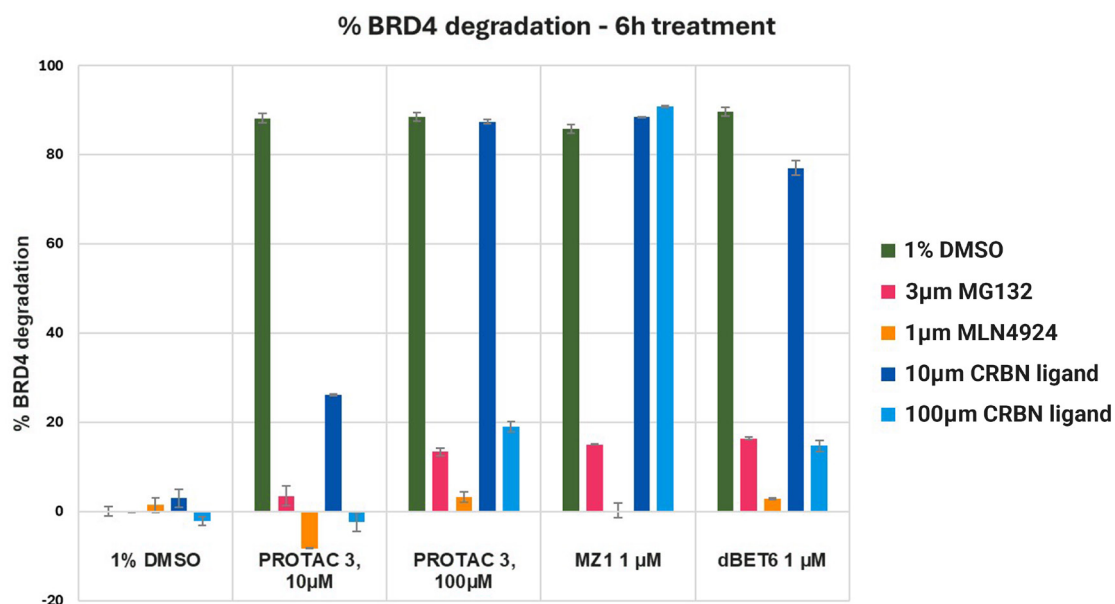


**Figure 11. Overview of the mechanism of action of CRBN-based PROTAC 3.** The bar plot illustrates ubiquitin recruitment and proteasome-mediated degradation of BRD4, assessed by an HTRF-based assay after 6h co-treatment of HeLa cells with PROTAC 3 and either MG132 (proteasome inhibitor), MLN4924 (neddylation inhibitor), or a CRBN ligand. Co-treatment with these inhibitors reduced or abolished BRD4 degradation, confirming that PROTAC 3 acts through a CRBN-dependent ubiquitin–proteasome pathway.

In conclusion, PROTAC efficacy depends on the formation of a stable, cooperative ternary complex between the target and the E3 ligase, with a lifetime sufficient for efficient ubiquitination (typically seconds to minutes). Correlation of ternary complex dissociation rates ( $k_{off}$ ) with half-maximal degradation concentrations ( $DC_{50}$ ) for the seven PROTACs indicates that the most efficient degraders—PROTACs 1, 2, 3, and 5—form the most stable ternary complexes with the slowest off-rates, whereas PROTAC 7 shows partial degradation and PROTACs 4 and 6 are largely inactive (Figure 12). Although PROTAC 6 appears as an outlier, its distinct binary binding profile with BRD4-BD1 suggests a different interaction mode with the target, highlighting that optimal PROTAC design is governed by a complex interplay of multiple factors. These results clearly demonstrate that linker chemistry not only modulates selectivity across different bromodomains but also influences both binary and ternary kinetics, ultimately impacting cellular degradation efficiency of BRD4-targeting PROTACs by quantifying endogenous BRD4 levels in HeLa cells.

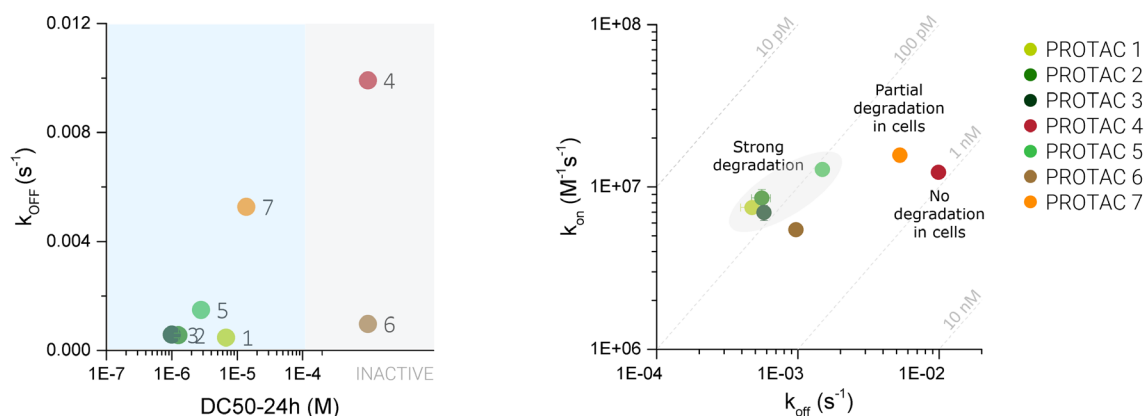


**Figure 12. Correlation of ternary complex kinetics and cellular degradation, and iso-affinity analysis for the PROTAC series.** Each point represents a PROTAC, showing the relationship between ternary complex dissociation rates ( $k_{off}$ ) and cellular degradation potency. Blue shading highlights active PROTACs inducing degradation, while grey indicates inactive compounds. Right: Kinetic rate map plotting mean  $k_{on}$  versus mean  $k_{off}$  values, with dashed iso-affinity lines corresponding to  $K_d = 0.01, 1, 10, \text{ and } 100 \text{ nM}$ .

## Conclusion

Using a BD1-biased DEL screening strategy, a BRD4 BD1-selective ligand with favorable physicochemical properties was identified and directly translated into a focused PROTAC series without further optimization of the warhead. Systematic variation of linker length and topology was shown to strongly influence CRBN engagement, ternary complex stability, and ultimately cellular degradation.

The multiplexed **Triceratops SPR #64** assay demonstrated the selectivity of the PROTAC designs toward BRD4, particularly the BD1 domain, and highlighted the critical role of binary ligase interactions in the overall degradation profile. **switchSENSE®** analyses further showed that efficient BRD4 degradation correlates with the formation of stable, long-lived ternary complexes, whereas shortened or rigid linkers led to altered binding modes, reduced ligase engagement, and weak or absent degradation. These observations were confirmed in cellular assays, where PROTACs 1, 2, 3, and 5 induced robust BRD4 degradation, with mechanistic studies validating CRBN- and proteasome-dependent activity for PROTAC 3. In contrast, PROTACs 4, 6, and 7 exhibited minimal or no cellular protein degradation.

## References

- [1] Doroshow, D.B. et al. (2017) 'BET inhibitors: a novel epigenetic approach', *Annals of Oncology*, 28(8).
- [2] Kong, N. R.; Jones, L. H. Clinical Translation of Targeted Protein Degraders. *Clin. Pharmacol. Ther.* 2023, 114 (3), 558–568. doi.org/10.1002/cpt.2985
- [3] Kroupova, A.; Spiteri, V. A.; Rutter, Z. J.; Furihata, H.; Darren, D.; Ramachandran, S.; Chakraborti, S.; Haubrich, K.; Pethe, J.; Gonzales, D.; Wijaya, A. J.; Rodriguez-Rios, M.; Sturbaut, M.; Lynch, D. M.; Farnaby, W.; Nakasone, M. A.; Zollman, D.; Ciulli, A. Design of a Cereblon Construct for Crystallographic and Biophysical Studies of Protein Degraders. *Nat. Commun.* 2024, 15 (1). doi.org/10.1038/s41467-024-52871-9.
- [4] BET Bromodomain Proteins Brd2, Brd3 and Brd4 Selectively Regulate Metabolic Pathways in the Pancreatic  $\beta$ -Cell
- [5] Deeney, J.T., Belkina, A.C., Shiriha, O.S., Corkey BE, Denis GV (2016) BET Bromodomain Proteins Brd2, Brd3 and Brd4 Selectively Regulate Metabolic Pathways in the Pancreatic  $\beta$ -Cell. *PLOS ONE* 11(3): e0151329. <https://doi.org/10.1371/journal.pone.0151329>.
- [6] Ponzo, I.; Solda, A.; Crowe, C.; Dahl, G.; Geschwindner, S.; Ciulli, A.; Rant, U. Proximity Biosensor Assay for PROTAC Ternary Complex Analysis. *ChemRxiv* March 6, 2024. doi.org/10.26434/chemrxiv-2024-8w4zb.
- [7] Wellaway, C.R. et al. (2020) 'Structure-based Design of a Bromodomain and Extraterminal Domain (BET) Inhibitor Selective for the N-terminal Bromodomains that Retains an Anti-inflammatory and Anti-proliferative Phenotype'.
- [8] Michael Zengerle, Kwok-Ho Chan, and Alessio Ciulli (2015) 'Selective Small Molecule Induced Degradation of the BET Bromodomain Protein BRD4' *ACS Chemical Biology*, 10, 8, 1770–1777.

Bruker Daltonics is continually improving its products and reserves the right to change specifications without notice. © Bruker Daltonics 01-2026, SPR-13, 1926955

For Research Use Only. Not for use in clinical diagnostic procedures.

### Bruker Switzerland AG

Fällanden · Switzerland  
Phone +41 44 825 91 11

### Bruker Scientific LLC

Billerica, MA · USA  
Phone +1 (978) 663-3660

